Development of Performance Parameters for the Assessment of Reinforced Concrete Bridge Girder Beams

Rudy Djamaluddin
Department of Civil Engineering, Faculty of Engineering, Hasanuddin University, Indonesia
rudy0011@gmail.com

Rusdi Usman Latief
Department of Civil Engineering, Faculty of Engineering, Hasanuddin University, Indonesia
rusdiusmanlatief@unhas.ac.id

Fakhruddin
Department of Civil Engineering, Faculty of Engineering, Hasanuddin University, Indonesia
fakhruddin@unhas.ac.id (corresponding author)

Kohei Yamaguchi
Department of Civil and Structural Engineering, Nagasaki University, Nagasaki, Japan
kohei@nagasaki.u.ac.jp

Arman Setiawan
Department of Civil Engineering, Faculty of Engineering, Hasanuddin University, Indonesia
arman.rafif.setiawan@gmail.com

Received: 27 October 2025 | Revised: 8 December 2025 and 20 December 2025 | Accepted: 21 December 2025

 DOI: https://doi.org/10.48084/etasr.15826

ABSTRACT

Bridge inspections typically involve complex measurement criteria and take a long time. This study proposes a simpler inspection method that assesses the performance of reinforced concrete bridge girder beams. The method relies on crack length correlation with beam performance using theoretical approaches, Finite Element Model (FEM) simulations, and experimental testing. A reinforced concrete beam model is used to simulate similar flexural behavior to that of actual bridge girders. The results show that cracks form when concrete stress exceeds rupture stress, usually at 8%-12% of the ultimate capacity. Cracks grow until the steel reinforcement yields, which happens around 80%-90% of the ultimate capacity. Experimental crack length data at ultimate capacity align closely with FEM simulations, with a ratio of 0.92. In contrast, the results differ significantly from the theoretical predictions, with a ratio of 1.54. The study introduces six performance levels for reinforced concrete beams, linking crack length to beam performance. These parameters will help estimate bridge girder performance through visual crack assessments.

Keywords-reinforced concrete beam; crack length; cracking; flexural performance; inspection; maintenance

I. INTRODUCTION

Reinforced concrete bridges are widely used for short- to medium-span applications due to the complementary behavior of concrete in compression and steel reinforcement in tension [1, 2]. Accordingly, several design standards have been established for reinforced concrete beams and bridge girders, including AASHTO LRFD, Eurocode 2, and related studies such as [3]. The development of reinforced concrete bridge infrastructure has increased the demand for systematic performance evaluation through regular inspections. However, in countries with extensive infrastructure growth, such as Indonesia, comprehensive inspections of all reinforced concrete bridges remain challenging due to limited resources, complex assessment criteria, and time-consuming procedures. Conventional bridge inspection methods often require detailed measurements and extensive fieldwork, which reduces their practical efficiency. Therefore, this study proposes a simplified

inspection approach to assess the performance of reinforced concrete bridge girder beams. The proposed method correlates crack length with structural performance levels, based on theoretical analysis, Finite Element Method (FEM) simulations, and experimental testing. A reinforced concrete beam model is adopted to represent the flexural behavior of reinforced concrete bridge girders, providing a practical basis for performance evaluation. The analysis method assumes a linear stress distribution and defines the ultimate strength once the section is fully cracked, thus failing to capture strain redistribution and progressive cracking [4, 5]. The FEM is a numerical method used to examine the behavior of structures and materials under various conditions in greater detail and more efficiently [5-7].

The FEM plays a crucial role in modeling, predicting, and validating the behavior of structures under both laboratory and field conditions. Through numerical simulation, FEM enables the identification of potential structural deficiencies prior to physical testing, thereby supporting more efficient and well-informed experimental design [8–11]. Furthermore, FEM results can be directly compared with experimental data to evaluate model accuracy and to better understand the influence of field conditions on structural performance [12, 13]. This research is significant because it provides a comprehensive framework for evaluating reinforced concrete beams by integrating theoretical analysis, FEM-based numerical simulation, and experimental testing. The primary objective of this study is to develop alternative performance indicators for reinforced concrete bridge girders. The combined use of manual calculations, laboratory experiments, and FEM analysis allows for a thorough understanding of the mechanical behavior of reinforced concrete beams throughout their loading stages. Based on this integrated approach, six distinct structural performance levels were defined, ranging from the initial elastic stage to cracking, yielding, and ultimate failure, thereby establishing a new evaluation framework applicable to both academic research and field-based monitoring. The relevance of the proposed performance parameters is further strengthened through verification against the design provisions of [14]. Consequently, the findings of this study contribute not only to academic advancement but also to practical applications, including the maintenance, rehabilitation, and safety enhancement of reinforced concrete infrastructure. This approach improves the accuracy of ultimate capacity estimation, enables detailed assessment of crack development under varying load levels, and provides insight into elastic–inelastic transitions and strain redistribution. As a result, it enhances model validation and supports more reliable performance-based assessment of reinforced concrete bridge girders under flexural loading.

II. THEORETICAL APPROACH

Reinforced concrete beams exhibit progressive changes in flexural behavior as the applied load increases, beginning with the occurrence of initial cracking, followed by the yielding of steel reinforcement, and continuing until ultimate capacity is reached. This behavior is illustrated in Figure 1. The stress–strain response of reinforced concrete beams can be divided into three distinct stages. Point A represents the initial cracking stage, which occurs when the tensile stress exceeds the tensile strength of concrete. Point B corresponds to the yielding of the steel reinforcement, characterized by a rapid increase in deformation with limited additional load. Point C denotes the crushing of concrete in the compression zone, leading to ultimate flexural failure. These stages correspond, respectively, to the cracking moment (*Mcr*), yield moment (*My*), and ultimate moment (*Mu*), as depicted in Figure 2.

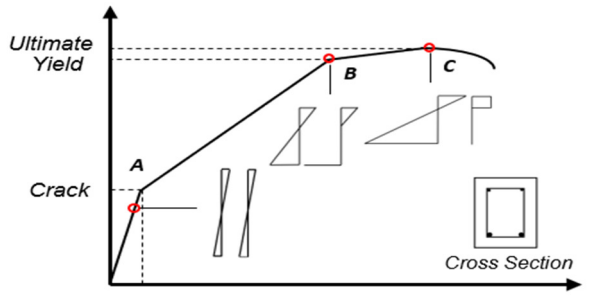

Fig. 1. Stress-strain curve.

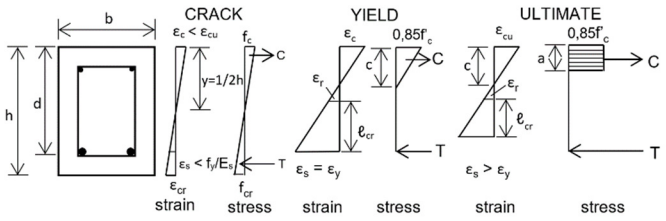

Fig. 2. Strain and stress distribution model at the crack, yield, and ultimate capacity.

Based on the strain distribution diagram, the flexural moment capacity of a reinforced concrete beam can be derived from the relationship between material strain parameters and crack length (l_{cr}). The mathematical expressions for the yield moment (M_y) and the ultimate moment (M_u) are:

$$M_y = A_s.f_y\left(d - \frac{\varepsilon_s(d-l_{cr})-\varepsilon_r.d}{3(\varepsilon_s-\varepsilon_r)}\right)$$

$$M_u = A_s.f_y\left(d - \frac{\beta_1.\varepsilon_{cu}(d-l_{cr})}{2(\varepsilon_r+\varepsilon_{cu})}\right)$$

For the condition at yielding moment M_y, the strain in the tensile reinforcement reaches the yield strain such that $\varepsilon_s = \varepsilon_y$. At the ultimate moment M_u, the behavior of the reinforcement continues in the plastic region where $\varepsilon_s > \varepsilon_y$. The term l_{cr} represents the crack length that develops in the tension zone of the beam owing to the flexural loading. The fracture strain of concrete is defined as $\varepsilon_r = \frac{f_r}{E_c}$, where f_r is the modulus of rupture and E_c is the modulus of elasticity of concrete, indicating the strain at cracking (rupture). The ultimate compressive strain of concrete was assumed to be $\varepsilon_{cu} = 0.003$ according to [14]. These equations are consistent with the stress-strain relationship shown in Figures 1 and 2. To validate the theoretical approach, calculations were performed to evaluate the flexural response considering the cracking, yield, and ultimate stages. The beam had dimensions of 150 mm × 200 mm with a span of 3000 mm reinforced by 3 D13 bars as

tensile reinforcement. The yield strength and concrete strength were 400 MPa and 25 MPa, respectively. The moment capacity and crack length ratio to effective depth *d* for the theoretical calculations are summarized in Table I.

TABLE I. THEORETICAL CALCULATION ANALYSIS RESULTS

Load level	Moment	Deflection	Steel strain	Concrete strain	Crack length (*lcr*)/*d*
	kN.m	mm	με	με	-
First crack	6.49	2.69	208	134	0
Yield	33.65	16.05	1573	1086	0.5
Ultimate	34.31	40.23	3390	3000	0.65

III. SPECIMEN AND METHODS

A. Specimens

The specimen was a 150 mm × 200 mm × 3300 mm concrete beam reinforced with 2D8 top bars, 3D13 bottom bars, and D8 stirrups, as detailed in [14-16], with proper cover ensured by spacers. The reinforcement layout and beam geometry are illustrated in Figure 3.

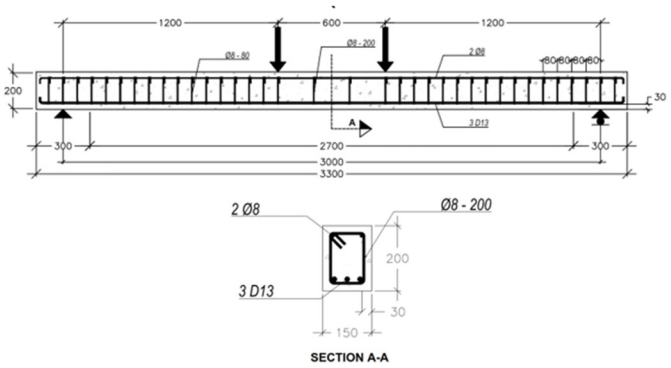

Fig. 3. Details of specimen beam.

B. Methods

This study comprised three stages: a theoretical analysis based on [14] to predict performance parameters, laboratory testing to obtain load–deflection behavior and crack patterns, and FEM simulations to model stress–deformation. This integrated approach aligns with the analytical, experimental, and numerical results. The laboratory test was performed using a hydraulic jack, as shown in Figure 4. Loading was applied incrementally under displacement control at a mid-span deflection rate of 0.2 mm/s, while the applied load was measured using a load cell. Force and displacement data were continuously recorded by a data logger, and the mid-span deflection was monitored using a Linear Variable Differential Transformer (LVDT).

Fig. 4. Test specimen setup.

For comparison, FEM simulations were also conducted. Material properties were defined with a concrete elastic modulus of 21.5 GPa and a steel modulus of 200 GPa by applying a concrete cracking model and an Elastoplastic steel model to assess the effect of reinforcement on beam performance. The finite element mesh of the reinforced concrete beam model is shown in Figure 5.

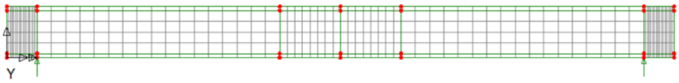

Fig. 5. Finite element mesh of the reinforced concrete beam model.

IV. RESULTS AND DISCUSSION

A. Material Test

The compressive and splitting tests of concrete, as well as the tensile tests of steel rebar, were conducted to identify the mechanical properties used in this study, as portrayed in Figure 6. According to [15], the Ø8 and D13 bars were classified as BjTP 280 and BjTS 420B, respectively. The concrete achieved an average compressive strength of 23.48 MPa and a splitting tensile strength of 2.2 MPa, respectively. The yield tensile strength of steel rebar was 408 MPa.

Fig. 6. Material strength tests.

B. Experimental Results

The results of a series of bending test specimens show a typical bending behavior of a reinforced concrete beam. Figure 7 presents a typical crack pattern of the tested beams. When the load is still relatively low, where the concrete's rupture stress has not been exceeded, no cracks are visible yet. When the load is applied such that the rupture stress is exceeded, cracks begin to appear, as illustrated in Figure 7(a). Based on the test results,

initial cracks start to emerge when the moment reaches approximately 8.5% of the ultimate moment. Under further loading, these cracks propagate lengthwise, extending upwards, accompanied by the appearance of new cracks. Based on observations, the cracks propagate rapidly until the steel reinforcement reaches its yield stress, as shown in Figure 7(b), while the reinforcement's yield stress occurs at approximately 90% of the ultimate capacity. Under further loading, the cracks do not develop significantly until they end with crushing of concrete in the compression zone (Figure 7(c)). The longest crack is the main crack that actively propagates upwards.

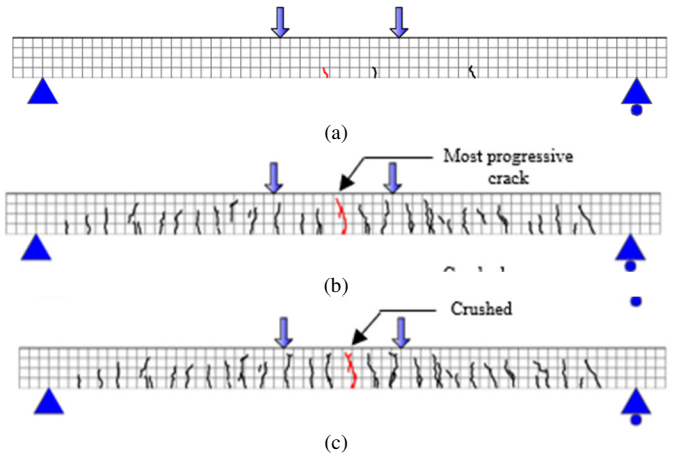

Fig. 7. Crack patterns at crack, yield, and ultimate load.

A summary of the average experimental test results, including the moment due to load, deflection, concrete strain, steel reinforcement strain, and crack length, is presented in Table II. The results indicate that cracks began to appear when the occurring moment was 3.1 kN·m, or 8.5% of the ultimate moment. The steel reinforcement reached yield strain when the moment acting on the beam was 33.3 kN·m, or approximately 91% of the ultimate moment capacity. At this point, the crack length was 160 mm, which is larger compared to the theoretical crack length, with a ratio of 1.9. This can be understood by the fact that theoretical calculations are performed based on assumptions such as the linearity of the strain diagram and the simplification of the stress diagram for reinforced concrete sections.

TABLE II. EXPERIMENTAL DATA RESULTS

Load level	Moment	Deflection	Steel strain	Concrete strain	Crack length	l_{cr}Exp/ l_{cr}Cal
	kN.m	mm	με	με	mm	-
First crack	3.1	1.06	73	86	0	0
Yield	33.3	18.80	2014	1307	160	1.9
Ultimate	36.4	49.04	>2014	3186	170	1.55

C. FEM

To perform a comparison with the experimental tests, a FEM-based model of the reinforced concrete beam was also conducted. The modeling of the concrete and steel reinforcement materials references common and widely used models, utilizing a non-linear analysis basis [17, 18]. The material properties used in the modeling refer to the material properties obtained from the experimental tests. Figure 8 shows the stress contours and crack indications at each concrete level: at the first cracking load, the load at reinforcement yield, and at the ultimate load. As can be observed, the FEM shows cracks developing from the initial cracking stage until the yielding of the reinforcement, accompanied by changes in stress within the beam model's cross-section. This aligns with the experimental test results.

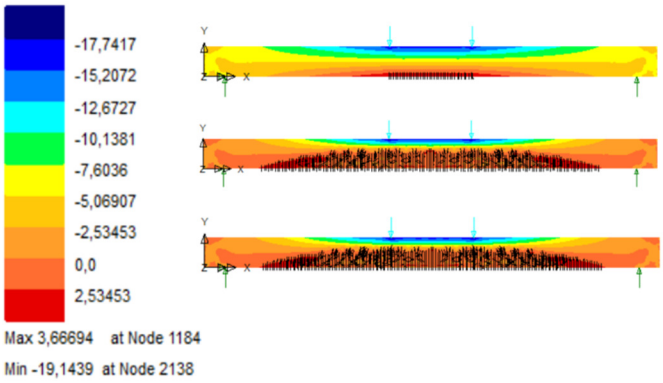

Fig. 8. Stress contour of the beam.

A summary of the reinforced concrete beam FEM results is presented in Table III. The results indicate that cracks began to appear when the occurring moment was 7.2 kN·m. The steel reinforcement reached yield strain when the moment acting on the beam was 28.3 kN·m, or approximately 89% of the ultimate moment capacity. The comparison of the FEM crack length with the experimental results at the point of reinforcement yield is 0.97, and at ultimate capacity is 0.92. This indicates a good agreement and confirms FEM as a reliable tool for predicting flexural behavior [19].

TABLE III. FEM ANALYSIS RESULTS

Load level	Moment	Deflection	Steel strain	Concrete strain	Crack length	l_{cr}Exp/l_{cr}FEM
	kN.m	mm	με	με	mm	-
First crack	7.2	3.59	174	127	0	0
Yield	28.3	17.62	1813	1940	165	0.97
Ultimate	31.9	46.05	2499	3296	184	0.92

D. Flexural Crack Behavior

Based on the discussion that has been carried out, it may be concluded that there is a relationship between the crack length and the moment occurring in a reinforced concrete beam cross-section as a representative example of a reinforced concrete beam in a bridge. When the moment is still relatively small, cracks are not yet apparent. Initial cracks begin to appear if the concrete rupture stress has been reached, which can occur when the moment reaches the range of 8%-12% of the ultimate moment. The addition of load will increase the moment, causing the cracks to propagate longitudinally upward, accompanied by the appearance of new cracks. The cracks propagate rapidly until the steel reinforcement reaches its yield stress, which occurs in the range of 80%-90% of the ultimate

capacity. Table IV summarizes the comparison of crack lengths at initial cracking, reinforcement yielding, and ultimate conditions.

TABLE IV. CRACK PROPAGATION RESULTS

Load level	l_{cr}Cal	l_{cr}Exp	l_{cr}FEM	l_{cr}Exp/ l_{cr}Cal	l_{cr}Exp/ l_{cr}FEM
	mm	mm	mm	-	-
Crack	0	0	0	0	0
Yield	84	160	165	1.9	0.97
Ultimate	110	170	184	1.55	0.92

E. Comparison of Experimental, FEM, and Theoretical Results

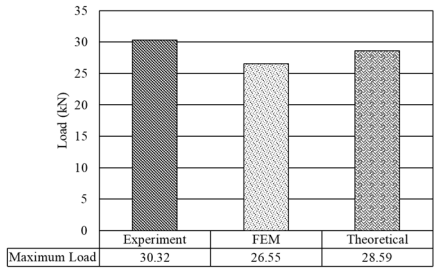

(a)

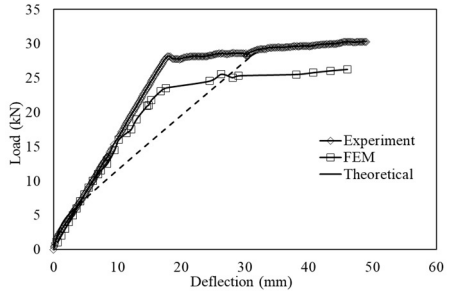

(b)

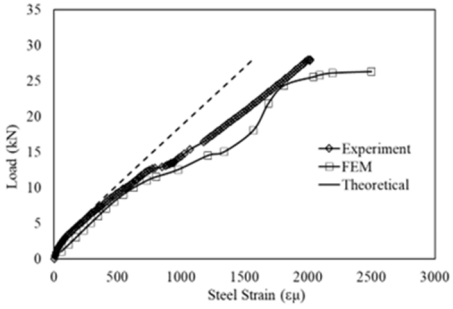

(c)

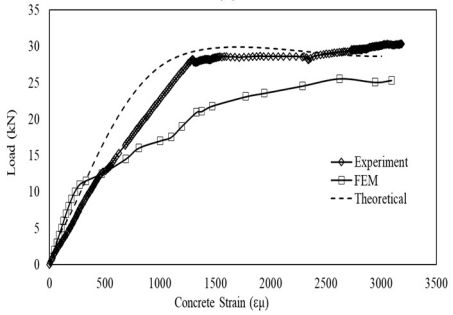

(d)

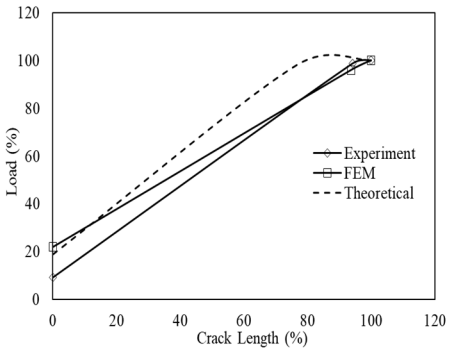

(e)

Fig. 9. Comparison of experimental, FEM, and theoretical results.

To evaluate the consistency among the experimental, FEM, and theoretical results, several key mechanical parameters governing the flexural behavior of reinforced concrete beams were examined. Figure 9 presents comparisons of ultimate capacity, deflection, steel tensile strain, and concrete compressive strain. Figure 9(a) shows that the ultimate capacity obtained from the experimental tests and FEM analysis agrees well with the theoretical predictions, with ratios of 1.06 and 0.93, respectively. Figures 9(b-d) display the load–deflection and load–strain relationships. These results show close agreement among all approaches within the elastic range. Minor discrepancies appear in the post-yield region, primarily due to idealized material assumptions in the numerical and theoretical models. Figure 9(e) illustrates the relationship between load and crack length and shows a similar progression across the experimental, FEM, and theoretical results. This confirms that both FEM simulations and theoretical calculations can capture the essential flexural response of reinforced concrete beams, despite some differences. A comparative assessment indicates that each approach exhibits distinct characteristics in predicting flexural behavior. Experimental results are used as the primary reference because they reflect actual beam behavior, including material variability and natural crack development. FEM modeling demonstrates excellent agreement with experimental data, particularly in predicting ultimate load capacity, deflection response, and crack propagation. However, the FEM response appears smoother due to the smeared crack representation. The theoretical analysis remains useful as a conservative estimation method but is less representative of the beam behavior in the post-cracking stage.

F. Proposed Performance Parameters

Based on the theoretical study, experimental results, and FEM simulations, the load–deflection behavior of reinforced concrete beams can be classified into six distinct performance levels, ranging from the initial service load to the ultimate stage. These levels capture the transition from elastic response and crack initiation to progressive cracking, yielding, and final failure, as depicted in Figure 10.

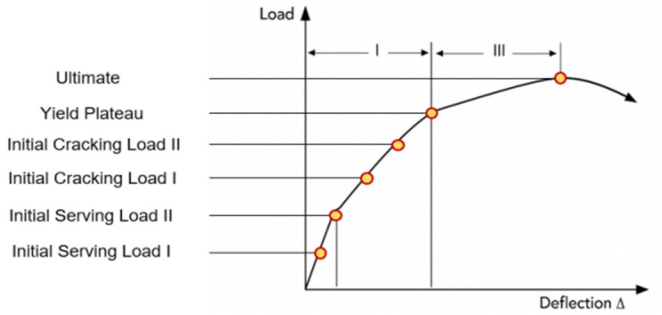

Fig. 10. Load level curve of reinforced concrete beam.

Each performance level is characterized by observable structural responses, such as deflection and crack development. Reinforced concrete beams typically remain uncracked when subjected to relatively low loads within the service load range. As the applied load increases and exceeds the tensile rupture strength of concrete, visible cracks begin to form, with crack length being the most readily observable indicator. With further loading, these cracks progressively propagate and increase in length until the beam reaches its ultimate capacity. Based on this behavior, the structural performance of reinforced concrete beams can be classified into six distinct performance levels. In general, these loading levels are described as follows:

- Initial Service Load I (Pre-linear Service): The structure remains elastic; reinforcement begins to carry load, with no visible damage and minimal deformation.
- Initial Service Load II (Crack Initiation): Microcracks initiated in the tensile zone as concrete tensile strength is exceeded, while the shear zone remains effective. It is assumed that concrete behaves in a linear elastic manner right up to this point for service load.
- Initial Cracking Load I (Progressive Cracking): Cracks propagate upward, stiffness decreases, deflection increases, and minor shear deformations appear.
- Initial Cracking Load II (Pre-Yield Transition): Stiffness decreases; reinforcement is fully engaged, stirrup shear strain rises, and nonlinear behavior emerges.
- Yield Plateau: Stiffness decreases significantly, and Plastic deformations dominate; shear cracks develop near supports, indicating strong flexural–shear interaction.
- Ultimate Load: Maximum capacity is reached; flexural and shear cracks merge, concrete crushing occurs, and failure becomes irreversible.

It should be noted that the proposed performance parameters are derived from analyses of the simulated beams, which are intended to represent the general behavior of reinforced concrete beams. Nevertheless, these parameters can be used as a practical reference for evaluating the performance of reinforced concrete beams in field applications. To support performance assessment based on visual inspection, particularly through observation of crack length, the mechanical performance parameters are organized into quantitative indicators. These indicators describe structural performance in terms of applied load level, crack length, and the extent of the cracked area, as summarized in Table V.

TABLE V. MECHANICAL PERFORMANCE PARAMETERS

Loading level	**Applied load (%)**	**Crack length (%)**	**Crack zone (%)**		**Structural performance parameters**	**Material response (steel and concrete)**	**Combined structural evaluation**
			Vertical	**Diagonal**			
Initial Service Load I (Prelinear Service)	0 – 9	0 – 3	0 – 2	–	Structure is still uncracked and in elastic behavior	Strain begins to appear in tensile reinforcement; concrete remains within elastic limits	Flexural and shear members are still functioning; no visual damage
Initial Service Load II (Crack Initiation)	10 – 19	4 – 22	3 – 4	–	Initial cracks appear	Initial cracks appear in the bottom tensile zone; concrete in the shear zone remains active	Early flexural damage signs; shear beams do not yet show structural symptoms
Initial Cracking Load I (Progressive Cracking)	20 – 40	23 – 30	5 – 12	–	Measured crack development	Tensile strain in the bottom reinforcement increases; the shear concrete begins to exhibit slight deformation	Cracks propagate upward; deformation becomes visible in the web
Initial Cracking Load II (Pre-Yield Transition)	41 – 96	31 – 50	13 – 35	–	Reduction in structural stiffness	Tensile reinforcement is fully engaged; shear strain increases; concrete weakens in tensile and web zones	Structure exhibits nonlinear behavior; weak regions begin to spread
Yield Plateau	91 – 99	73 – 93	42 – 54	0 – 28	Significant deformation is visible	Plastic strain is predominantly observed in the bottom tensile reinforcement; shear strain is mainly concentrated in the stirrups (shear reinforcement); the concrete and web experience damage due to shear forces	Vertical and shear cracks develop simultaneously; deformation in the web; support becomes integrated
Ultimate	100	100	>60	>28	Structural collapse	Maximum strain occurs in the bottom tensile reinforcement and shear reinforcement; failure due to the combined action of shear and flexure is inevitable	The structure reaches the threshold of local collapse; deformation becomes irreversible; the shear zone is crushed

V. CONCLUSIONS

Based on the above results, it can be concluded that crack length development under different loading levels provides a clear and measurable representation of the structural performance of reinforced concrete beams. As the applied load increases, cracks propagate progressively, reflecting the successive stages of structural response from service conditions to ultimate failure. These results confirm that crack characteristics, particularly crack length and propagation, can serve as reliable indicators of structural performance. The novelty of this research lies in the development of crack-based performance parameters classified into six distinct performance levels. This approach offers a practical alternative to conventional evaluation methods, which typically rely primarily on strength capacity or deflection criteria. The main contribution of this study is the introduction of a simple, visually based, and potentially field-applicable framework for assessing the performance of reinforced concrete beams during structural inspections. Nevertheless, to enhance the reliability and general applicability of the proposed performance parameters, further studies involving larger-scale specimens and validation through field investigations are required.

ACKNOWLEDGMENT

The authors would like to extend their deepest appreciation to Hasanuddin University Research and Community Service Institutions for their financial support of this research. They also thank the Structures and Materials Laboratory of Hasanuddin University for their invaluable support and constructive input throughout the preparation of this research, which was essential to the successful completion of this work. In addition, the authors appreciate the advice of the Structure and Bridge Laboratory of Nagasaki University.

REFERENCES

[1] L. Moya and E. O. L. Lantsoght, "Parametric Study on the Applicability of AASHTO LRFD for Simply Supported Reinforced Concrete Skewed Slab Bridges," *Infrastructures*, vol. 6, no. 6, June 2021, Art. no. 68, https://doi.org/10.3390/infrastructures6060088.

[2] F. E. Ame, J. N. Mwero, and C. K. Kabubo, "Openings Effect on the Performance of Reinforced Concrete Beams Loaded in Bending and Shear," *Engineering, Technology & Applied Science Research*, vol. 10, no. 2, pp. 5352–5360, Apr. 2020, https://doi.org/10.48084/etasr.3317.

[3] D. Essen and N. Hidayah, "Comparative Analysis of Plate Girder Designs on Non-Composite Bridges Between AASHTO LRFD Bridge Design Specifications 2017 Code With SNI 1729:2015 Code," *Neutron*, vol. 20, pp. 16–32, July 2020, https://doi.org/10.29138/neutron.v20i01.45.

[4] A. A. Alomari, "Investigation of spacing limits for crack control reinforcement within AASHTO LRFD strut-and-tie modeling design provisions," Dec. 2022, [Online]. Available: https://repositories.lib.utexas.edu/items/145158b9-e529-4d84-a9dd-919cc7583892.

[5] D. De Domenico, N. Spinella, D. Messina, M. Mazzeo, and A. Recupero, "Structural behavior of deteriorated Gerber half-joints in highway overpasses by nonlinear finite element analysis combined with a simplified uniform-corrosion model," *Structural Concrete*, vol. 26, no. 5, pp. 5677–5707, 2025, https://doi.org/10.1002/suco.202400556.

[6] S. Rahman and M. Haque, "Experimental Investigation and Finite Element Analysis of Reinforced Concrete Rectangular Beam," *Proceedings of 4th International Conference on Advances in Civil Engineering 2018 (ICACE 2018)*, pp. 410–415, Dec. 2018.

[7] A. A. Mahmoud, B. K. El Gani, T. S. Mustafa, and A. N. M. Khater, "Experimental, Numerical, and Analytical Investigation of the Reinforced Concrete Hidden and Wide Beams," *International Journal of Concrete Structures and Materials*, vol. 18, no. 1, Oct. 2024, Art. no. 73, https://doi.org/10.1186/s40069-024-00709-5.

[8] M. Anghileri and F. Biondini, "Experimental validation of nonlinear finite element analysis of PC bridge deck beams based on the results of full-scale load tests," in *Life-Cycle of Structures and Infrastructure Systems*, CRC Press, 2023.

[9] I. Singh, N. Dev, S. Pal, and T. Visalakshi, "Finite Element Analysis of Impact Load on Reinforced Concrete," in *CIGOS 2021, Emerging Technologies and Applications for Green Infrastructure*, Singapore, 2022, pp. 265–274, https://doi.org/10.1007/978-981-16-7160-9_26.

[10] A. Kheyroddin and A. Mortezaei, "Nonlinear Finite Element Analysis of Reinforced Concrete Bridges," *Journal of Transportation Research*, vol. 3, no. 4, Jan. 2007 Art. no. e11366.

[11] H. Sebastian, A. Lisantono, Y. Arfiadi, J. Utomo, and R. Frans, "The Load-Carrying Capacity of Reinforced Concrete Beam to Beam Connection: An Experimental Program," in *ARPHA Proceedings*, Oct. 2024, vol. 7, pp. 216–223, https://doi.org/10.3897/ap.7.e0216.

[12] O. C. Zienkiewicz and R. L. Taylor, *The Finite Element Method*, 1st ed. USA: Butterworth Heinemann, 2000.

[13] Oñate, *Structural Analysis with the Finite Element Method*. Dordrecht: Springer Netherlands, 2009.

[14] *SNI 2847-2019 Persyaratan Beton Struktural Untuk Bangunan Gedung dan penjelasan*. Indonesia: Standar Nasional Indonesia, 2019.

[15] *SNI 2052:2017 Baja tulangan beton*. Indonesia: Standar Nasional Indonesia, 2017.

[16] *SNI 6880:2016 Spesifikasi beton struktural*. Indonesia: Standar Nasional Indonesia, 2016.

[17] M. Keintjem, R. Suwondo, and M. Suangga, "Finite Element Based Optimization of Two-Way Concrete Slabs: A Comparative Study on Embodied Carbon and Cost Efficiency," *Engineering, Technology & Applied Science Research*, vol. 15, no. 4, pp. 25251–25256, Aug. 2025, https://doi.org/10.48084/etasr.11607.

[18] H. A. Elgohary, "Comparative reliability analysis of punching shear design for edge column-flat slab connections without shear reinforcement," *Journal of Umm Al-Qura University for Engineering and Architecture*, vol. 16, no. 3, pp. 682–693, Sept. 2025, https://doi.org/10.1007/s43995-025-00158-5.

[19] H. A. Elgohary, "A simplified trilinear concrete stress–strain curve: energy-based modeling of experimental data compliant with various codes," *Journal of Umm Al-Qura University for Engineering and Architecture*, vol. 16, no. 2, pp. 443–453, June 2025, https://doi.org/10.1007/s43995-025-00117-0.